Influence of pressure on the magnetic ordering of CeNiSnH and $CeNiSnH_{1.8}$ hydrides

2009 J. Phys.: Condens. Matter 21 305601

(http://iopscience.iop.org/0953-8984/21/30/305601)

J. Phys.: Condens. Matter **21** (2009) 305601 (7pp) doi:10.1088/0953-8984/21/30/305601

Influence of pressure on the magnetic ordering of CeNiSnH and $CeNiSnH_{1.8}$ hydrides

J Rodriguez Fernandez[1], S F Matar[2], D P Rojas[1], L Torralbo-Campo[1] and B Chevalier[2,3]

[1] CITIMAC, Facultad de Ciencias, Universidad de Cantabria, 39005 Santander, Spain
[2] CNRS, Université de Bordeaux, ICMCB, 87 Avenue du Docteur Albert Schweitzer, 33608 Pessac Cedex, France

E-mail: chevalie@icmcb-bordeaux.cnrs.fr

Received 6 March 2009, in final form 2 June 2009
Published 6 July 2009
Online at stacks.iop.org/JPhysCM/21/305601

Abstract

The magnetic properties of the antiferromagnet CeNiSnH and of the ferromagnet $CeNiSnH_{1.8}$ on hydrostatic pressure ($0 \leqslant P \leqslant 10.8$ bar) have been determined using a miniature piston–cylinder CuBe pressure cell. With increasing P, the Néel temperature of CeNiSnH increases weakly from 4.77 to 5.01 K whereas the Curie temperature of $CeNiSnH_{1.8}$ decreases rapidly from 7.16 to 5.30 K. Similar pressure dependence is also observed in the critical field of the metamagnetic transition of CeNiSnH and in the coercive field of $CeNiSnH_{1.8}$. Electronic structure calculations for these hydrides within the density functional theory show agreement with the experimental findings. Detailed examination of the chemical bonding features point to the conclusion that the antibonding Ce–Ni states below the Fermi level for $CeNiSnH_{1.8}$ could be responsible for the decrease of its Curie temperature under applied pressure.

(Some figures in this article are in colour only in the electronic version)

1. Introduction

Recently, it was established that the ternary stannide CeNiSn, a so-called Kondo semiconductor and classified as a strongly correlated f-electron system, absorbs hydrogen [1–4]. Exposed at 523 K to 1 MPa of hydrogen gas, this compound transforms to the hydride $CeNiSnH_{1.8}$, which decomposes at the same temperature but under low hydrogen pressure (5×10^{-3} MPa) into another hydride CeNiSnH [1, 3]. The last hydride crystallizes, as CeNiSn in the orthorhombic ε-TiNiSi type [2], whereas $CeNiSnH_{1.8}$ belongs to the hexagonal ZrBeSi-type structure [1]. H insertion leads to an increase of the unit cell volume, respectively, of 2.6 and 8.0% per mole with increasing H content. The crystal structures of CeNiSn, CeNiSnH and $CeNiSnH_{1.8}$ present some similarities [5]. The cerium three-dimensional network can be described by an intergrowth of trigonal [Ce_6] prisms surrounding alternatively the Ni and Sn atoms. However, these [Ce_6] prisms are distorted in CeNiSn and CeNiSnH. Besides, Ni- and Sn atoms form a hexagonal network, which is respectively buckled in CeNiSn and CeNiSnH and regular in $CeNiSnH_{1.8}$. Thus, in the two hydrides, the H atoms are located inside the [Ce_3Ni] tetrahedral sites. In $CeNiSnH_{1.8}$ nearly all the tetrahedra that are identical, are occupied [1]. In contrast, in CeNiSnH two types of chemically similar but geometrically different [Ce_3Ni] tetrahedra are formed; only the one that has a nearly regular Ce_3 side is occupied by a hydrogen atom [2].

Magnetic ordering is induced by the hydrogenation of CeNiSn. CeNiSnH is antiferromagnetic below $T_N = 4.5$ K whereas $CeNiSnH_{1.8}$ exhibits a ferromagnetic behaviour with $T_C = 7.0$ K as Curie temperature [1, 2, 6]. It is worth noting that the variation of volume induced by H insertion promotes magnetic ordering for the compounds deriving from CeNiSn. Hydrogenation, which decreases the c–f hybridization between the 4f(Ce) electrons and the conduction electrons, acts as application of a 'negative' pressure on intermetallics. Similar results are obtained by substitution of Cu, Pd or Pt for Ni in CeNiSn; the unit cell volume increases and the non-

[3] Author to whom any correspondence should be addressed.

magnetic ground state is transformed into an antiferromagnetic state [7–10]. All these behaviours indicate that the physical properties of CeNiSn are very sensitive to the volume effects.

Investigation of the hydrides $CeNiSnH_x$ by electrical resistivity and specific heat measurements reveals a marked influence of the Kondo interactions [6]. For instance, the electrical resistivity ρ of $CeNiSnH_{1.8}$ increases in a Kondo-like manner when the temperature decreases from 270 to about 25 K [1, 6]. This behaviour is characteristic of incoherent Kondo scattering with a $\rho = -A \log T$ (A = constant) dependence. The influence of the Kondo effect is less marked on the electrical resistivity of the other hydride CeNiSnH; its curve $\rho = f(T)$ exhibits only a curvature between 25 and 300 K [6]. Also, the analysis of the specific heat data C_p in the paramagnetic range up to 20 K using the $C_p/T = f(T^2)$ plot yields for $CeNiSnH_{1.8}$ an electronic coefficient $\gamma =$ 184 mJ K^{-2} mol^{-1} larger than that corresponding to CeNiSnH ($\gamma =$ 39 mJ K^{-2} mol^{-1}) [6]. Moreover, the magnetic entropy associated with the magnetic ordering of the two hydrides reaches only 0.54 R Ln 2, which is substantially reduced from R Ln 2 = 5.76 J mol^{-1} K^{-1}, the value expected for a doublet ground state of the Ce^{3+} ion. This reduction of the magnetic entropy is interpreted as due to the Kondo interactions [11].

In this context, it was useful to perform magnetization measurements under pressure on the hydrides CeNiSnH and $CeNiSnH_{1.8}$ in order to determine the evolution of their magnetic ordering temperature. It is well known that the physical properties of the magnetic Kondo lattices described by Doniach's phase diagram are strongly influenced by the pressure [12]. In some cases, as for CePdSb or CeAg, the ferromagnetic properties can be completely destroyed by the application of pressure [13]. In this paper, we present and discuss the pressure dependence of the T_N and T_C temperatures respectively of the hydrides CeNiSnH and $CeNiSnH_{1.8}$. The different evolutions detected (T_N increases whereas T_C decreases with increasing pressure) are discussed in connection with a theoretical study by first principles calculations on the electronic structure of $CeNiSnH_x$ hydrides.

2. Experimental and computational details

CeNiSnH and $CeNiSnH_{1.8}$ samples used for this study were synthesized and characterized by x-ray powder diffraction as described previously in [1, 3]. The hydrides are stable in air and their H content is not affected by exposure under vacuum for temperature smaller than 300 K.

A miniature piston–cylinder CuBe pressure cell has been used for magnetization measurements in a commercial (Quantum Design) SQUID magnetometer. The pressure was determined at low temperatures using the known pressure dependence of the critical temperature of the superconducting state of a Sn sensor placed inside the cell. The empty pressure cell was measured separately and the signal corrected accordingly. The magnetization versus temperature, $M = f(T)$, and magnetic field, $M = f(H)$, have been measured under hydrostatic pressures up to 10.8 kbar value (at ~3.5 K) in the temperature range 2–12 K and in magnetic fields up to 50 kOe.

For a detailed description of the electronic band structure of the ternary stannide CeNiSn and its hydrides, we use all electron calculations based on the density functional theory (DFT) framework [14, 15] as built within the scalar relativistic augmented spherical wave (ASW) method [16]. Effects of exchange and interactions were accounted for with a local density approximation (LDA) scheme [17]. In order to check for the limitations of the LDA, we have performed full-potential ASW LDA + U calculations for $CeNiSnH_x$ hydrides using values of $U = 6.7$ eV and $J = 0.7$ eV acting on 4f(Ce) states. As a result, the changes are rather small especially for the magnitudes of the magnetic moments and result in an upshift of the 4f(Ce) states within the conduction band. This gives sufficient confidence for our use of an LDA scheme in the present study and to consider 4f(Ce) states within the valence basis set. In recent years, we have shown that this framework is well adapted to determine the electronic and magnetic structures of the hydrides based on cerium [18–21]. The wavefunction is expanded in atom-centred augmented spherical waves, which are Hankel functions and numerical solutions of Schrödinger's equation, respectively, outside and inside the so-called augmentation spheres. In order to optimize the basis set, additional augmented spherical waves within IS (interstitial spheres) were placed at carefully selected interstitial sites with s, p, and d symmetry. The choice of these sites as well as the augmentation radii was automatically determined using the sphere-geometry optimization algorithm [22]. All valence electrons, including 4f(Ce), were treated as band states. In the minimal ASW basis set, we chose the outermost shells to represent the valence states and the matrix elements were constructed using partial waves up to $l_{max} + 1 = 4$ for Ce, $l_{max} + 1 = 3$ for Ni, $l_{max} + 1 = 2$ for Sn and $l_{max} + 1 = 1$ for H. The completeness of the valence basis set—without calling for semicore states—was checked at all volumes for charge convergence with $l_{max} + 1$ occupation less than 0.1 electrons. Regarding the angular momentum expansions, they are in principle carried to infinity. The self-consistent field calculations are run to a charge convergence of $\Delta Q \sim 10^{-8}$ and the accuracy of the method is in the range of about 0.1–1 meV regarding energy differences. A sufficiently large number of k points was used to sample the irreducible wedge of the Brillouin zone, i.e., respectively 1024 and 576 irreducible k points generated from 4096 points ($16 \times 16 \times 16$) for the orthorhombic (CeNiSnH) and hexagonal ($CeNiSnH_{1.8}$) structures under study. All calculations were firstly carried out assuming neutral atomic species in a non-magnetic configuration (non-spin-polarized, NSP), meaning that spin degeneracy was enforced for all species. Note that such a configuration does not refer to a paramagnet, which would only be simulated by large super-cells entering random spin orientations over the different magnetic sites. NSP calculations provide a description of the system as a function of energy positions of the site projected density of states DOS as well as an assessment of the chemical bonding. These are derived here based on the overlap populations (S_{ij}) within the COOP (crystal orbital overlap population) criterion [23]. This is related to the fact that the spin polarized bands result

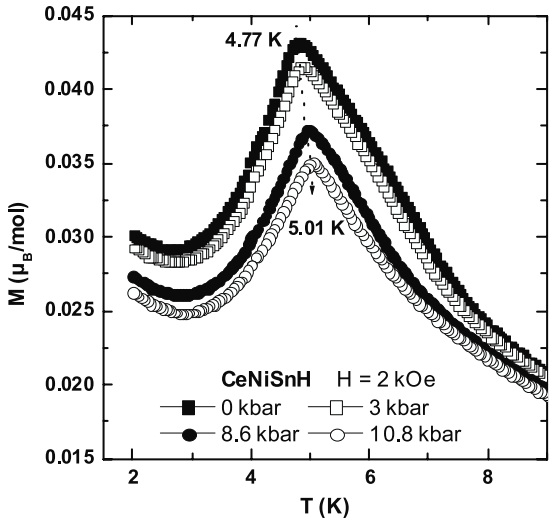

Figure 1. Temperature dependence of magnetization, measured with an applied field $H = 2$ kOe and under various external pressures, for CeNiSnH.

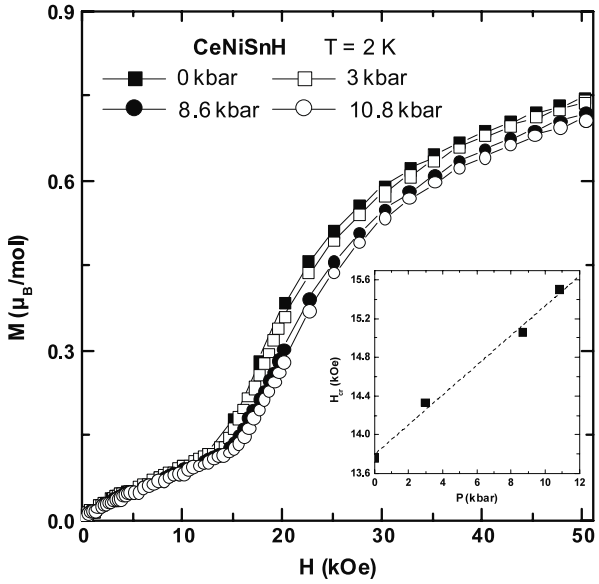

Figure 2. Field dependence at 2 K and under various external pressures of the magnetization of CeNiSnH. The inset presents the pressure dependence of the critical field H_{cr} characterizing the metamagnetic transition.

from the NSP bands by a rigid energy shift. While this is the case of the ternary stannide CeNiSn and the hydrides under consideration (cf figure 8), it needs to be noted that some magnetic systems characterized by so-called 'covalent magnetism' [24, 25] do not show the same weight of majority spin (↑) and minority spin (↓) density of states (DOS). For such systems, it can be expected that the chemical bonding is spin dependent. Then subsequent spin polarized calculations check for the actual ground state of the two hydrides.

3. Results and discussion

3.1. Magnetization versus pressure

Figure 1 presents, at low temperatures, the influence of pressure P on the magnetization M of the hydride CeNiSnH. For $P = 0$ kbar, the curve $M = f(T)$ exhibits a maximum near 4.77 K; this behaviour agrees with the occurrence of an antiferromagnetic ordering for this hydride [3, 6, 26]. With increasing P, the maximum shifts to higher temperatures. For $P = 10.8$ bar, the Néel temperature is estimated at 5.01 K. The pressure also influences the metamagnetic transition evidenced previously for CeNiSnH (figure 2) [3]. The critical field H_{cr} where this transition appears increases linearly with P, as indicated in the inset of figure 2, H_{cr} varying between 13.8 and 15.5 kOe when P increases from ambient pressure to 10.8 bar. This investigation indicates that the antiferromagnetic behaviour of CeNiSnH is reinforced by the external pressure.

Figure 3 shows the thermal dependence of the magnetization M of $CeNiSnH_{1.8}$ measured under various pressures P and an applied field H of 2 kOe. All these curves $M = f(T)$ present a strong increase of M characterizing the occurrence of a ferromagnetic ordering. At $P = 0$ kbar, the Curie temperature T_C, determined from the inflection point of the curve $M = f(T)$, equals 7.16 K; a value comparable to that reported previously [1]. The T_C temperature is dependent on P; T_C varies between 7.16 and 5.30 K when P increases from

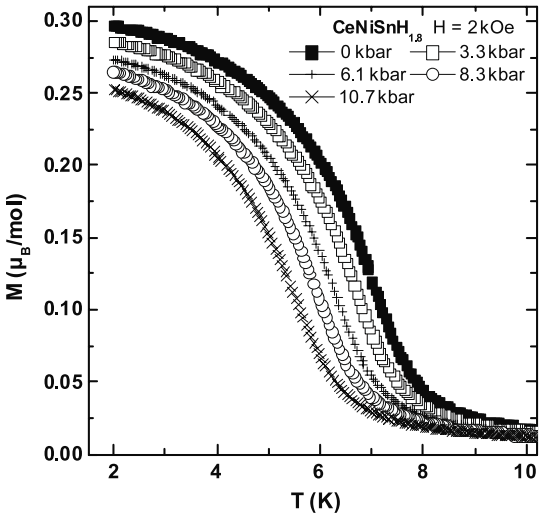

Figure 3. Temperature dependence of magnetization, measured with an applied field $H = 2$ kOe and under various external pressures, for $CeNiSnH_{1.8}$.

0 to 10.7 kbar. The isothermal magnetization measurements performed at 2 K (figure 4) confirm this ordering, but (i) the magnetization at 50 kOe (figure 4(a)) and the remanence (figure 4(b)) decrease with increasing P; for instance, this remanence takes the values 0.27 and 0.19 μ_B mol^{-1} when P increases from 0 to 10.7 kbar; and (ii) the coercive field H_c also decreases with increasing P; moreover, H_c varies linearly with P (inset of figure 4(b)). In other words, the ferromagnetic character of the hydride $CeNiSnH_{1.8}$ is diminished by application of the external pressure.

Figure 5 compares the pressure dependence of the magnetic ordering temperatures of the hydrides CeNiSnH and $CeNiSnH_{1.8}$. Between $P = 0$ and 10.8 kbar, T_N of

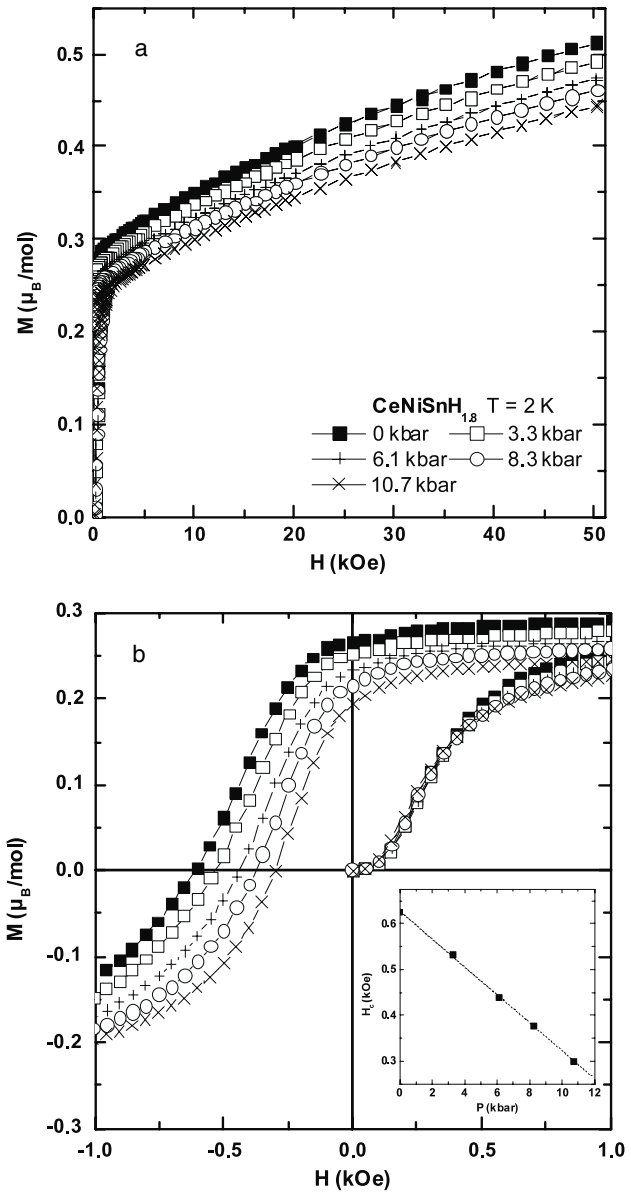

Figure 4. Field dependence at 2 K of the magnetization of $CeNiSnH_{1.8}$, measured under various external pressures and for magnetic field (a) 0 kOe $\leqslant H \leqslant$ 50 kOe and (b) -1 kOe $\leqslant H \leqslant$ 1 kOe. The inset of (b) shows the pressure dependence of the coercive field H_c.

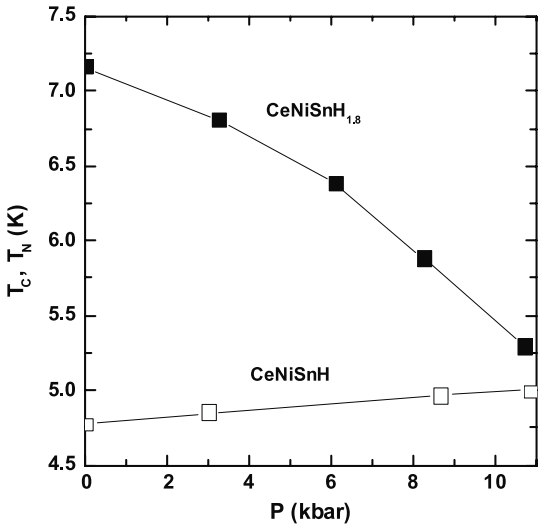

Figure 5. Pressure dependence of T_N and T_C ordering temperatures respectively for the hydrides CeNiSnH and $CeNiSnH_{1.8}$.

CeNiSnH increases weakly (4.77 $\rightarrow$ 5.01 K) whereas T_C of $CeNiSnH_{1.8}$ decreases more strongly (7.16 $\rightarrow$ 5.3 K). These opposite evolutions can be discussed on the basis of Doniach's phase diagram describing the competition between T_{RKKY} (indirect magnetic RKKY interaction) and T_K (Kondo effect) temperatures depending on the coupling constant J_{cf} between 4f(Ce) and conduction electrons [13, 27]. Considering that the increase of P leads to an enlargement of J_{cf}, the dependence of T_N and T_C on P suggests that (i) CeNiSnH is a magnetic RKKY metal (the left part of Doniach's phase diagram) whereas (ii) $CeNiSnH_{1.8}$ is a magnetic Kondo system (middle part of the diagram). The influence of P on the Kondo effect can also be evaluated considering the direct relation between T_K and the paramagnetic Curie temperature θ_P ($T_K \sim |\theta_P|$) [11]. In this sense, the analysis of the reciprocal magnetic susceptibility $\chi_m^{-1} = f(T)$ above 100 K shows a slight increase, from $|\theta_P| = 19$ K ($P = 0$) to $|\theta_P| = 23$ K ($P = 10.8$ kbar), for CeNiSnH. However, in the other hydride, $CeNiSnH_{1.8}$, $|\theta_P|$ not only is higher, but also exhibits a stronger pressure dependence, changing from $|\theta_P| = 106$ K ($P =$ 0 kbar) to $|\theta_P| = 134$ K ($P = 10.7$ kbar). Considering all these facts, the influence of the Kondo effect on the magnetic properties is higher in the $CeNiSnH_{1.8}$ hydride. In this view, it is interesting to investigate the electronic structures of these two hydrides deriving from CeNiSn.

3.2. Density of states and chemical bonding

At self-consistent convergence charge transfer is found from the atomic species toward the IS with a redistribution of the electrons over the valence states due to quantum mixing between them. The site projected DOS for the two hydrides CeNiSnH and $CeNiSnH_2$ (full occupancy by H atom of the $4f$ site in the $P6_3/mmc$ space group [5]) are shown in figure 6. In this plot as well as in the following ones, the zero energy is with respect to the Fermi level E_F. The nearly twice as large DOS magnitude for CeNiSnH is due to the twice as large number of formula units per cell in its orthorhombic cell with respect to the two formula units in the hexagonal $CeNiSnH_2$ hydride. At E_F the major feature is the crossing at a relatively large intensity of the 4f(Ce) states. The 4f band is mainly found and centred within the conduction band due to the low filling of the 4f(Ce) states already in the atomic state but is found here to be close to one, 1.1 for CeNiSnH and 1.38 for $CeNiSnH_2$, thus pointing to Ce^{3+} character. This agrees with a former investigation on these hydrides by Aburto *et al* [28]. The corresponding density of states at E_F, $n(E_F)$, amounts to 49 Ryd^{-1} and 81 Ryd^{-1} for CeNiSnH and $CeNiSnH_2$, respectively. In this context the corresponding value for the pristine CeNiSn stannide is $\sim$28 Ryd^{-1}. The increase of $n(E_F)$ from CeNiSnH to $CeNiSnH_2$ is in agreement with that of the

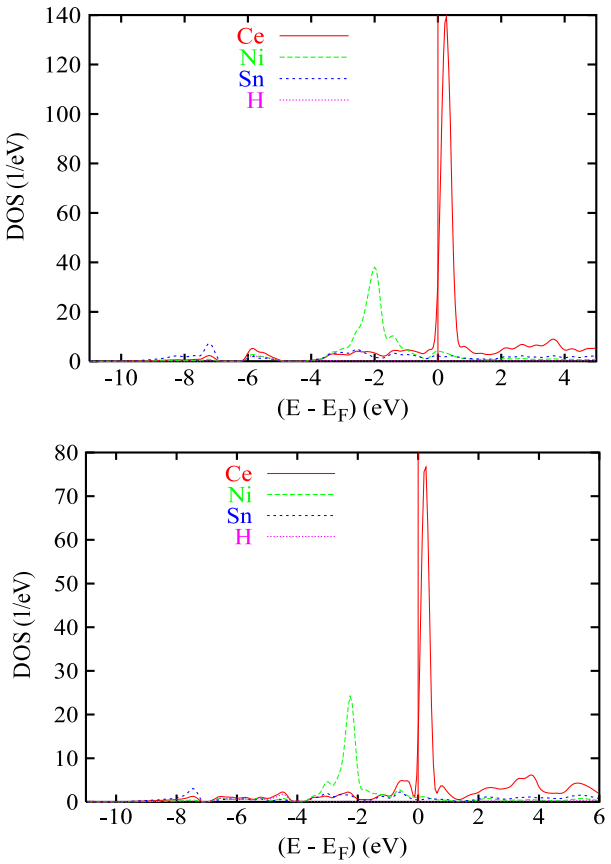

Figure 6. Site projected density of states for the hydrides CeNiSnH (top) and $CeNiSnH_2$ (bottom).

electronic coefficient γ (39 $\rightarrow$ 184 mJ K^{-2} mol^{-1}) evidenced by specific heat measurement [6] however one cannot expect an agreement for the magnitudes as the calculations provide the electronic part only while in experiment the electron phonon interaction is additionally accounted for.

The $n(E_F)$ values can be analysed within the Stoner mean field theory of band ferromagnetism [29], which is a mean field treatment. For a coexistent Kondo state and magnetic ordering, a mean field approach was equally used by Irkhin *et al* [30]. Despite the 'localized' nature of the Kondo lattice one can still deal with the alloy systems in the framework of an itinerant model of magnetism so that the mean field treatment within the Stoner model can be valid at least to establish trends. This model predicts the system to be unstable in a non-magnetic state if it is characterized by a large $n(E_F)$ resolved for a given atomic constituent, here mainly 4f(Ce). This is expressed by the unit-less Stoner product: $I \cdot n(E_F)$, which can be either larger or smaller than one depending on whether the system will be unstable in a spin-degenerate, non-magnetic configuration or not, respectively. I is the Stoner integral obtained from spin polarized calculation of the relevant constituent, here cerium. From a former investigation devoted to the magnetic ordered intermetallic systems based on cerium [31], I(Ce) = 0.02 Ryd. The resulting Stoner products are then 0.98 and 1.6 for CeNiSnH and $CeNiSnH_2$, respectively, while a value of 0.56 is found for the pristine CeNiSn compound. Thus one may expect CeNiSnH to be on the verge of magnetic instability while $CeNiSnH_2$ should polarize magnetically with a finite magnetic moment. Such a feature was indeed observed by Aburto *et al* [28], who found CeNiSnH to behave as a weakly magnetic system with a small 4f(Ce) moment (0.28 μ_B) while $CeNiSnH_2$ had a much larger moment of 0.85 μ_B, respectively. However, these authors find a magnetic moment in CeNiSn, in contrast to experimental observations and present mean field theory results. It is interesting to note that the increase of the Stoner product in the sequence CeNiSnH $\rightarrow$ $CeNiSnH_2$ explains the higher magnetic ordering temperature of $CeNiSnH_2$ (T_C = 7.16 K) than that observed for CeNiSnH (T_N = 4.77 K); however, care should be taken as such a statement may not be generalized. In fact, according to the extended Stoner theory a sharp peak at E_F will give a high Stoner parameter but low moments and magnetic energy corresponding to low T_C, but if the same peak is broadened e.g. by structural changes the Stoner parameter will be lower but the moment and T_C will be higher.

Within the valence band (VB) there is a non-negligible contribution from cerium itinerant states below E_F, which is responsible for the chemical bonding with other constituents. Due to the large filling of their d states, Ni DOS are found completely within the VB around -2 eV. Low magnitude Sn s and p-like states are observed throughout the VB; they show similar peak shapes not only with Ni, but with Ce as well. This points to the hybridization between them through the chemical bonding. When H is introduced, the VB has extra states that are added through the redistribution of H s states over the available valence basis sets of neighbouring atoms. Their quantum mixing is better illustrated from the COOP below.

Using the overlap integral S_{ij} between two species i and j, we illustrate the chemical bonding properties. Besides volume expansion simulating a negative pressure, changes brought by hydrogen uptake within CeNiSn are likely to bring changes of the interactions between the lattice constituents. Figure 7 illustrates these bonding characteristics based on the COOP introduced above. Along the y-axis, positive, negative and zero COOP correspond to bonding, antibonding and non-bonding interactions, respectively. A lowering of the bonding from CeNiSnH to $CeNiSnH_2$ can be observed for Ce–Ni as well as for Ni–Sn interactions. This is due to the expansion of the unit cell due to H uptake leading to larger separations between the constituents. For both hydrides, the major part of VB is found to be bonding for Ce–Sn due to the small filling of 4f(Ce) states, i.e. extra electrons go into bonding states, in contrast to Ni–Sn, where the large filling of Ni d states leads to the occurrence of antibonding states below E_F for both hydrides. The main difference between the two hydrides is in the character of the Ce–Ni interaction, which is bonding over the VB in CeNiSnH and starts to have an antibonding character in the close neighbourhood of E_F. This is somehow opposite to the $CeNiSnH_2$ hydride, where Ce–Ni is bonding in the -4, -2 eV energy range but antibonding up to E_F. In fact, due to the electron brought by one extra H, E_F is 'pushed' up in energy and antibonding Ce–Ni states are found. This is likely to be destabilizing for the system, especially when external pressure is applied, i.e. E_F will cross antibonding states over a wide energy range in the $CeNiSnH_2$ hydride.

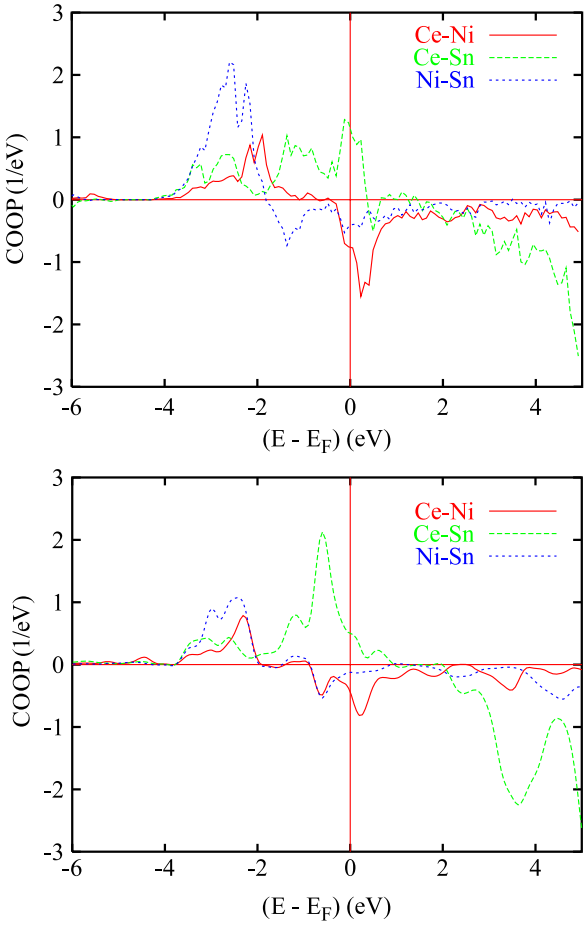

Figure 7. Atom-to-atom chemical bonding with COOP criterion for Ce–Ni, Ce–Sn and Ni–Sn interactions in CeNiSnH (top) and $CeNiSnH_2$ (bottom).

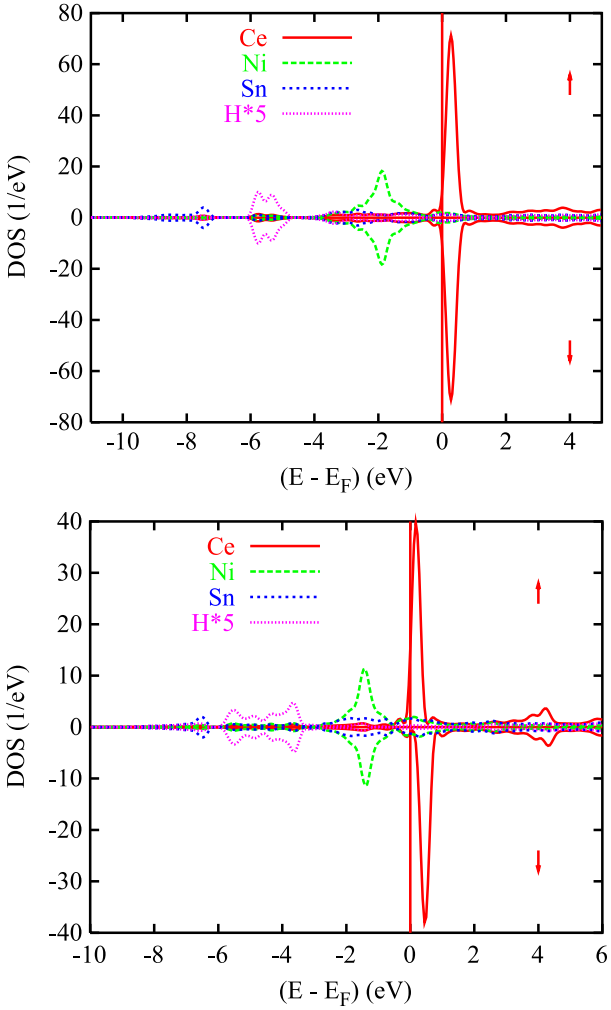

Figure 8. Spin polarized ferromagnetic configuration: site and spin projected density of states for the hydrides CeNiSnH (top) and $CeNiSnH_2$ (bottom).

We propose this feature to address the large changes of its ferromagnetic behaviour, especially for the weakening of the magnetic interactions, opposite to the CeNiSnH hydride, as presented in figure 5.

Lastly, spin polarized calculations were carried out to check the validity of the Stoner mean field analysis. This is done by allowing for two spin populations for both hydrides starting from converged NSP configurations above. Using the same self-consistent convergence criteria, the results show a total zero magnetization for CeNiSnH and a magnetization of 1.02 μ_B per unit cell for $CeNiSnH_2$. These results comply with the Stoner theory analysis above. In $CeNiSnH_2$, the cell magnetization is further decomposed unto the atomic moments (spin only): $m_{Ce} = 0.46\ \mu_B$, $m_{Ni} = 0.04\ \mu_B$, $m_{Sn} = 0.01\ \mu_B$ and $m_H = -0.001\ \mu_B$. However, one can expect the actual magnetization to arise mainly from Ce, i.e. the moments of the other constituents are consequent to the quantum mixing, which results in larger moment for Ni, which is a d element than for Sn (p element) or H (s element). The corresponding site and spin projected DOS are shown in figure 8. While for CeNiSnH there is no energy shift between (↑) and (↓) spin populations, an energy shift characterizes $CeNiSnH_2$. This is mainly observed for Ce DOS, where the energy difference between the band middles of (↑) and (↓) spins comes close to 0.5 eV and corresponds to magnetic exchange.

4. Conclusion

The magnetic properties of the hydrides deriving from the ternary stannide CeNiSn are differently influenced by the applied pressure P. With increasing P, the Néel temperature of CeNiSnH increases weakly whereas the Curie temperature of $CeNiSnH_{1.8}$ decreases significantly. In the same way, the critical field of the metamagnetic transition increases in CeNiSnH whereas the coercive field in $CeNiSnH_{1.8}$ decreases. Electronic structure calculations for hydrides $CeNiSnH_x$ within the density functional theory (DFT) explain their magnetic properties: (i) the density of states $n(E_F)$ at the Fermi level increases in the sequence CeNiSn → CeNiSnH → $CeNiSnH_{1.8}$ (or $CeNiSnH_2$) leading toward a transition from a Kondo semiconducting behaviour to a magnetically ordered hydride; (ii) the Stoner product $I \cdot n(E_F)$ is higher for the hydride $CeNiSnH_{1.8}$ (or $CeNiSnH_2$) showing the higher magnetic ordering temperature and (iii) finally the occurrence of antibonding Ce–Ni states below the Fermi level E_F for this last hydride could be responsible for the decrease of its Curie temperature under applied pressure.

Acknowledgments

This work was financially supported by the European Science Foundation (ECOMCOST action P16). The pressure experiments were supported by Spanish CICYT MAT2005-06806-C04 and MAT2008-06542-C04. Computation facilities were provided within the intensive numerical simulation facilities network M3PEC-Mesocentre of the University Bordeaux1.

References

[1] Chevalier B, Bobet J-L, Pasturel M, Bauer E, Weill F, Decourt R and Etourneau J 2003 *Chem. Mater.* **15** 2181
[2] Yartys V A, Ouladdiaf B, Isnard O, Khyzhun O Yu and Buschow K H J 2003 *J. Alloys Compounds* **359** 62
[3] Chevalier B, Pasturel M, Bobet J-L, Decourt R, Etourneau J, Isnard O, Sanchez Marcos J and Rodriguez Fernandez J 2004 *J. Alloys Compounds* **383** 4
[4] Stange M, Paul-Boncour V, Latroche M, Percheron-Guégan A, Isnard O and Yartys V A 2005 *J. Alloys Compounds* **404** 144
[5] Chevalier B, Wattiaux A, Fournès L and Pasturel M 2004 *Solid State Sci.* **6** 573
[6] Chevalier B, Pasturel M, Bobet J-L, Etourneau J, Isnard O, Sanchez Marcos J and Rodriguez Fernandez J 2004 *J. Magn. Magn. Mater.* **272–276** 576
[7] Takabatake T, Nakazawa Y, Ishikawa M, Sakakibara T, Koga K and Oguro I 1988 *J. Magn. Magn. Mater.* **76/77** 87
[8] Kasaya M, Tani T, Suzuki H, Ohoyama K and Kohgi M 1991 *J. Phys. Soc. Japan* **60** 2542
[9] Nishigori S, Goshima H, Suzuki T, Fujita T, Nakamoto G, Takabatake T, Fujii H and Sakurai J 1993 *Physica* B **186–188** 406
[10] Nishigori S, Goshima H, Suzuki T, Fujita T, Nakamoto G, Tanaka H, Takabatake T and Fujii H 1996 *J. Phys. Soc. Japan* **65** 2614
[11] Blanco J A, de Podesta M, Espeso J I, Gomez Sal J C, Lester C, McEwen K A, Patrikios N and Rodriguez Fernandez J 1994 *Phys. Rev.* B **49** 15126
[12] Larrea J, Fontes M B, Alvarenga A D, Baggio-Saitovitch E M, Burghardt T, Eichler A and Continentino M A 2005 *Phys. Rev.* B **72** 035129
[13] Cornelius A L, Gangopadhyay A K, Schilling J S and Assmus W 1997 *Phys. Rev.* B **55** 14109
[14] Hohenberg P and Kohn W 1964 *Phys. Rev.* B **136** 864
[15] Kohn W and Sham L J 1965 *Phys. Rev.* A **140** 1133
[16] Williams A R, Kübler J and Gelatt C D 1979 *Phys. Rev.* B **19** 6094
Eyert V 2007 *The Augmented Spherical Wave Method—a Comprehensive Treatment* (*Springer Lecture Notes in Physics* vol 719) (Berlin: Springer)
[17] Vosko S H, Wilk L and Nusair M 1980 *Can. J. Phys.* **58** 1200
[18] Matar S F 2007 *Phys. Rev.* B **75** 104422
[19] Chevalier B and Matar S F 2004 *Phys. Rev.* B **70** 174408
[20] Matar S F, Chevalier B, Eyert V and Etourneau J 2003 *Solid State Sci.* **5** 1385
[21] Chevalier B, Gaudin E, Al Alam A F, Matar S F, Weill F, Heying B and Pöttgen R 2008 *Z. Naturf.* b **63** 685
[22] Eyert V and Höck K-H 1998 *Phys. Rev.* B **57** 12727
[23] Hoffmann R 1987 *Angew. Chem. Int. Edn Engl.* **26** 846
[24] Williams A R, Zeller R, Moruzzi V L, Gelatt C D Jr and Kübler J 1981 *J. Appl. Phys.* **52** 2067
[25] Matar S F, Houari A, Belkhir M A and Zakhour M 2007 *Z. Naturf.* b **62** 881
[26] Sanchez Marcos J, Rodriguez Fernandez J and Chevalier B 2007 *J. Magn. Magn. Mater.* **310** 383
[27] Chevalier B, Wattiaux A and Bobet J-L 2006 *J. Phys.: Condens. Matter* **18** 1743
[28] Aburto A and Orgaz E 2007 *Phys. Rev.* B **75** 045130
[29] Mohn P 2003 *Magnetism in the Solid State, an Introduction* (Berlin: Springer)
[30] Irkhin Yu V and Katnelson M I 1990 *J. Phys.: Condens. Matter* **2** 8715
[31] Matar S F and Mavromaras A 2000 *J. Solid State Chem.* **149** 449